LAWRENCE
LIVERMORE
NATIONAL
LABORATORY

LLNL-PROC-413087

K-(alpha) X-ray Thomson Scattering From Dense Plasmas

A. L. Kritcher, P. Neumayer, J. Castor, T. Doppner, R. W. Falcone, O. L. Landen, H. J. Lee, R. W. Lee, E. C. Morse, A. Ng, S. Pollaine, D. Price, S. H. Glenzer

May 18, 2009

16th International Conference on Atomic Processes in Plasmas
Monterey, CA, United States
March 22, 2009 through March 26, 2009

Disclaimer

K-α X-ray Thomson Scattering From Dense Plasmas

Andrea L. Kritcher[a,b], Paul Neumayer[b], John Castor[b], Tilo Döppner[b], Roger W. Falcone[c], Otto L. Landen[b], Hae Ja Lee[c], Richard W. Lee[b,c], Edward C. Morse[a], Andrew Ng[b], Steve Pollaine[b], Dwight Price[b], Siegfried H. Glenzer[b]

[a]*Nuclear Engineering Department, University of California Berkeley, Berkeley, CA 94709, USA*
[b]*Lawrence Livermore National Laboratory, P.O. Box 808, Livermore, CA 94551, USA.*
[c]*Physics Department, University of California Berkeley, Berkeley, CA 94709, USA.*

Abstract. Spectrally resolved Thomson scattering using ultra-fast K-α x rays has measured the compression and heating of shocked compressed matter. The evolution and coalescence of two shock waves traveling through a solid density LiH target were characterized by the elastic scattering component. The density and temperature at shock coalescence, 2.2 eV and $1.7 \times 10^{23} cm^{-3}$, were determined from the plasmon frequency shift and the relative intensity of the elastic and inelastic scattering features in the collective scattering regime. The observation of plasmon scattering at coalescence indicates a transition to the dense metallic state in LiH. The density and temperature regimes accessed in these experiments are relevant for inertial confinement fusion experiments and for the study of planetary formation.

Keywords: X-ray scattering, Rayleigh, Thomson scattering, plasmon, dense plasmas.
PACS: 01.30.Cc

INTRODUCTION

The understanding of warm dense plasmas is important for several fields of research including planetary formation [1] and the modeling of planetary composition [2,3]. The study of shock wave heating in light elements, such as H and He, under high pressure conditions is also important for inertial confinement fusion experiments [4] such as on the future National Ignition Facility (NIF) [5], LLNL. Theories in this regime are not fully understood, and experimental data is necessary to test dense matter modeling. X-ray Thomson scattering has been developed as a dense matter diagnostic to determine the temperature, density, and ionization state of warm dense matter [6-8]. These first experiments from isochorically heated matter, employed Ly-α and He-α x-ray sources to probe the collective and non-collective plasma regimes.

More recently, experiments have measured the temperature and density of shocked-compressed matter [9-11], important for inertial confinement fusion experiments where deuterium-tritium filled capsules will be compressed by more than a factor of 1000 using a sequence of coalescing shock waves. New x-ray scattering experiments summarized in this paper that employ ultrafast K-α x-ray bursts [11] with a temporal

resolution of 10 ps [12] and bandwidth of $\Delta E/E=0.3\%$ have the additional advantage of high temporal and spectral resolution of the scattered spectra. With the use of these picosecond diagnostics, a snapshot of the material conditions can be probed during compression, allowing tests of dense matter modeling that is dependent on the material equation of state (EOS).

EXPERIMENTAL SETUP

These experiments were preformed at the Titan laser facility [13], where Ti K-α probe x-rays were produced via laser irradiation of a solid density Ti foil and a second 6 ns-long drive beam was used to shock-compress solid density LiH targets (1.9 x 3 x 0.3 mm, ρ_o=0.78g/cc), see Fig. 1 for a schematic of the experimental configuration. The nearly mono-energetic Ti K-α x-rays ($\Delta E/E$ = 0.3%) were produced from short-pulse laser irradiation (300 J, 1053 nm, 5 ps) of a 10 μm thick Ti foil. Two planar shocks were launched into the LiH by a shaped 6 ns-long drive beam (450 J, 527 nm, 2ω), with an intensity of $I=1x10^{13}$ Wcm^{-2} in a 4 ns long foot, followed by an intensity of $I=3x10^{13}$ Wcm^{-2} in a 2 ns long high intensity peak, see Fig. 2 for the drive and probe beam waveforms. For a smooth drive beam intensity profile, a 600 μm phase plate was used.

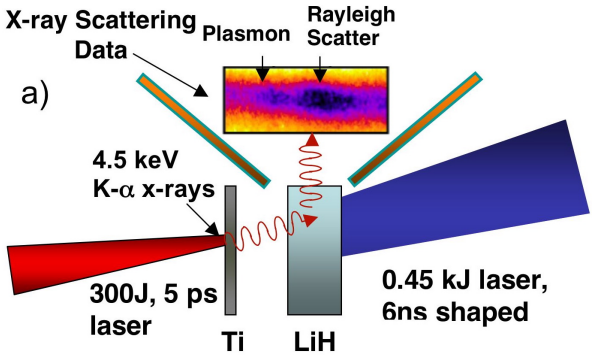

FIGURE 1. Schematic of the experimental configuration. Ultrafast (10 ps), nearly mono-energetic ($\Delta E/E < 0.3\%$) laser produced Ti K-α x rays (4.5 keV) are scattered from LiH targets that are compressed using a second 6 ns long shaped drive beam. A Highly Oriented Pyrolytic Graphite Bragg (HOPG) spectrometer is used to collect and disperse the scattered radiation. Gold shields restricted the view of the source and blow-off plasmas to the spectrometer.

A large (24 x 70 mm) cylindrically curved Highly Oriented Pyrolytic Graphite (HOPG) Bragg spectrometer was used to collect the scattered radiation side-on to the LiH targets, at a scattering angle of 40 ± 10^0. Image plate (IP) detectors were used to record the dispersed radiation. Gold shields (10 x 7.5 x 0.025 mm) were used to block the view of the source and blow-off plasmas to the scattering spectrometer. Figure 2 shows the calculated mass density of the compressed LiH using a 1D Lagrangian radiation-hydrodynamic modeling code HELIOS [14], as a function of target thickness and time since the start of the drive beam. For these calculations, the experimental long-pulse drive beam waveform was used as an input for the simulations. Radiation-

hydrodynamic modeling in this regime was weakly dependent on the details of radiation transport and heat conduction. Shock coalescence is predicted to occur at about 7 ns after the start of the drive beam, when a compression of about three times solid density is predicted. This experiment was designed to probe these target conditions.

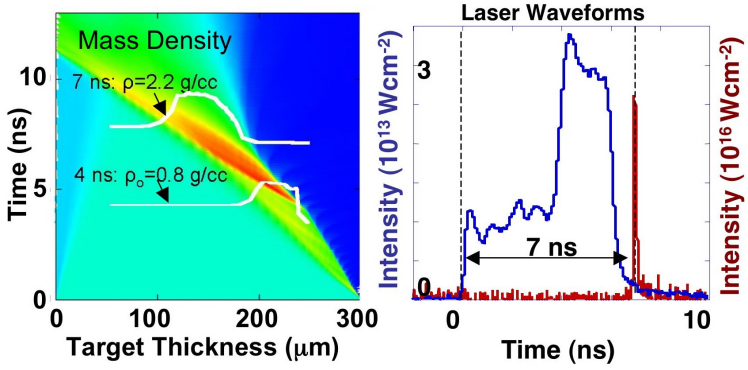

FIGURE 2. Radiation-hydrodynamic modeling of the mass density (left), plotted as a function of target thickness and time, where t=0 ns denotes the start of the drive beam. On the right are waveform profiles of the drive (blue) and probe (red) beams. The shaped drive beam first drove a slow shock into the material, with a low-intensity ($1x10^{13}$ Wcm^{-2}) 4 ns-long foot, and a second stronger shock into the target, with a high intensity ($3x10^{13}$ Wcm^{-2}) 2 ns-long peak.

RESULTS AND DISCUSSION

Raw experimental data and profiles of the scattered spectra are shown in Figures 3 and 4, respectively. Scattering just before the launch of the second strong shock wave (t = 4 ns) is dominated by elastic scattering and little to no inelastic scattering indicates a low ionization state in the plasma. Here, scattering from bound electrons and electrons that dynamically follow the ion motion results in an elastic Rayleigh scattering component. Scattering at shock coalescence (t = 7 ns) shows inelastic and elastic scattering features from interaction with free and bound electrons. The collective plasmon scattering feature [6], or inelastic feature, is a result of plasma (Langmuir wave) [15] oscillations by free (delocalized) electrons.

Theoretical fits to the scattering data at t= 4ns accounts for scattering from free, bound, and weakly bound electrons, and provides an upper limit on the degree of ionization, $Z^* < 0.2$. The elastic scattering intensity at t= 4 ns compared to scattering from heated LiH at t=7 ns indicates temperatures of < 0.4 eV. Scattering measurements at t=7 ns show strong inelastic scattering from plasmon oscillations, downshifted from the elastic scattering feature by ΔE_{pl}=24 eV, which provides an accurate measurement of the electron density ($1.7x10^{23}cm^{-3}$ ±10%), from the dispersion relation. For the temperatures probed in this experiment, correction to the dispersion relation due to thermal motion of the electrons was negligible, providing an accurate measure of the electron density.

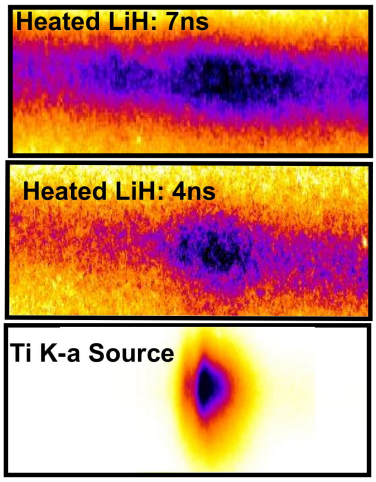

FIGURE 3. Measured x-ray scattering data using a HOPG spectrometer and image plate (IP) detector. The Ti K-α source (bottom), measured with the scattering spectrometer, shows no satellites on the red-wing, allowing accurate measurement of the downshifted plasmon feature. Scattering at t=4 ns (middle) ns before launch of the second strong shock, showed little inelastic scattering, indicating low temperature and ionization state. Scattering at t=7 ns (top) at coalescence of the two shocks shows plasmon scattering, which indicates a transition to a dense metallic state in LiH.

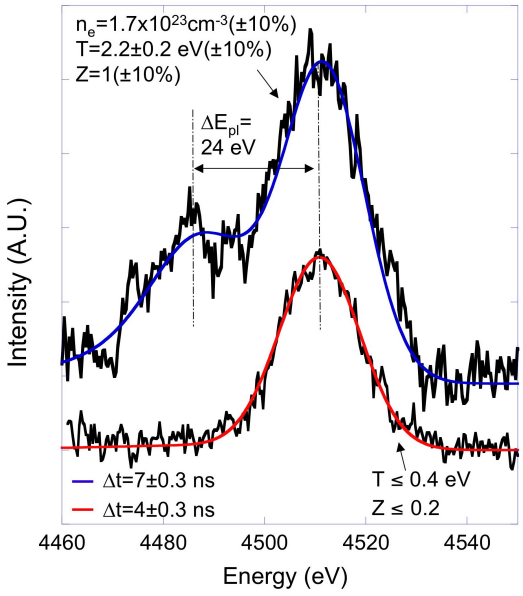

FIGURE 4. Profiles of the measured Thomson scattered spectra plotted with theoretical fits to the experimental data. Before the launch of the second strong shock (t=4 ns) (bottom), the spectrum is dominated by elastic scattering, indicating low temperature and ionization state. At shock coalescence (t = 7 ns) (top), an energy shift (24 eV) of the plasmon feature indicates 3x compression, while the intensity of the elastic scattering feature indicates heating to temperatures of 2.2 eV. The observation of plasmon scattering at t = 7 ns indicates a transition to the metallic free electron plasma state in solid density LiH.

Theoretical fits [16] of the elastic scattering intensity, relative to the inelastic scattering intensity, indicate a temperature of 2.2 eV with ±10% error in theoretical fitting to the experimental data. An ionization state of Z*=1 for Li(+)H is determined from the shape and intensity of the inelastic scattering peak with an error of ±10% from theoretical fitting to the experimental data. With measurement of the electron density and ionization state, a material compression of a factor of three (ρ/ρ_0=3) at coalescence was determined.

Data also show a rapid increase in elastic scattering at t = 7 ns compared to measurements taken earlier during shock compression that indicates rapid heating and shock coalescence. The theoretical models (SOCP) used to determine the temperature from dependence of the elastic scattering component on structure factor values, were tested in new separate experiments under similar material conditions [17]. These experiments measured the elastic scattering component as a function of wave vector, where the elastic scattering intensities were calibrated from inelastic scattering in the collective and non-collective regimes

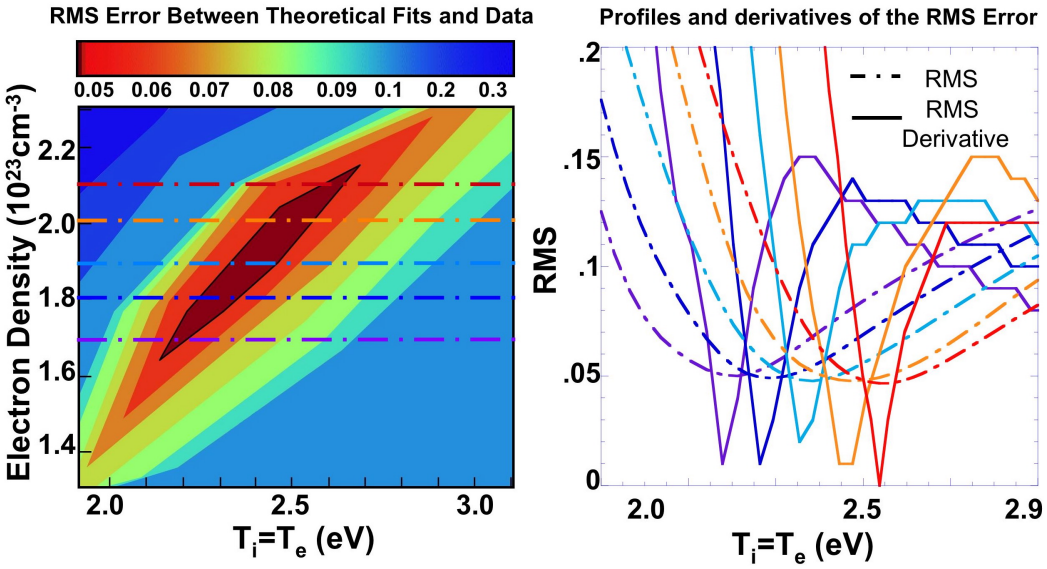

FIGURE 5. (Left) Sensitivity of theoretical scattering calculations to the experimental data for varying temperatures (T_e=T_i) and electron densities. Root Mean Squared (RMS) values are color coded for a range of temperature and density combinations, for an ionization state of Z*=1, where the centered black island is a range of possible best fits. The error of this fitting method to the experimental data is about ± 10% for the temperature and electron density. (Right) Profiles of the RMS contour (dashed lines, corresponding to the dashed lines on the contour plot) and derivatives of the RMS profiles (solid lines) which shows sensitivity of the change in RMS error.

Figure 5 shows RMS differences in theoretical fitting to the experimental data for a range of temperatures and densities used in the calculation. The dark-colored island in the center of the plot indicates a range of best theoretical fitting with ±10 % error in the temperature and electron density. Also plotted in Fig. 5 are profiles of the

RMS differences, at specific densities, corresponding to the dashed lines on the contour plot, and their derivatives to show sensitivity of change in RMS error as a function of temperature. Sensitivity of theoretical fitting to the experimental data show that plasma parameters can be determined simultaneously and with high accuracy for single shot characterization.

CONCLUSIONS

We have successfully demonstrated K-α X-ray Thomson scattering, enabling 10 ps temporal resolution for the characterization of shock compressed, solid density matter. A transition to the dense metallic plasma state in solid density material has been observed, resulting in the measurement of plasmons. The energy shift of the plasmon feature determined a compression of a factor of three times solid density at shock coalescence. At coalescence, a temperature (2.2 eV) was determined from the elastic scattering intensity relative to the inelastic scattering feature, accessing the warm dense matter regime. Measurement of the compression and heating of multi-shocked material provides a test for radiation-hydrodynamic models that are dependent on choice of EOS. This technique is opportune for inertial confinement fusion experiments, such as the National Ignition Facility [5], that will achieve extreme density conditions and require high temporal resolution for characterization of short lived states of compression, and can be used to test radiation hydrodynamic models.

ACKNOWLEDGMENTS

This work performed under the auspices of the U.S. Department of Energy by Lawrence Livermore National Laboratory under Contract No. DE-AC52-07NA27344. Work was also supported by the National Laboratory User Facility, Laboratory Directed Research and Development Grants No. 08-ERI-002 and No. 08-LW- 004, by the Helmholtz association (VH-VI-104) and by the Deutsche Forschungsgemeinschaft (SFB 652).

REFERENCES

1. H. C. Connolly and Jr., Stanley G. Love, Science **280**, 62 (1998).
2. T. Guillot, Science **286**, 72 (1999).
3. Nadine Nettelmann, Bastian Holst, Andre Kietzmann, Martin French, Ronald Redmer and David Blaschke, Astrophysics. J., **683**, 1217 (2008).
4. J. D. Lindl, Peter Amendt, Richard L. Berger, S. Gail Glendinning, Siegfried H. Glenzer, Steven W. Haan, Robert L. Kauffman, Otto L. Landen, and Laurence J. Suter, Phys. Plasmas **11**, 339. (2004).
5. J. D. Zuegel, S. Borneis, C. Barty, B. Legarrec, C. Danson, N. Miyanaga, P. K. Rambo, C. Leblanc, T. J. Kessler, A. W. Schmid, L. J. Waxer, J. H. Kelly, B. Kruschwitz, R. Jungquist, E. Moses, J. Britten, I. Jovanovic, J. Dawson, and N. Blanchot, Fusion Science and Tech. **49,** 453-482 (2006).
6. S. H. Glenzer, O. L. Landen, P. Neumayer, R. W. Lee, K. Widmann, S. W. Pollaine, R. J. Wallace, G. Gregori, A. Höll, T. Bornath, R. Thiele, V. Schwarz, W.-D. Kraeft, and R. Redmer, Phys. Rev. Lett. **98**, 065002 (2007).
7. S. H. Glenzer *et al.,* Phys. Rev. Lett. **90**, 175002 (2003), *ibid* Phys. Plasmas **10**, 2433 (2003).

8. G. Gregori *et al.,* Phys. Plasmas **11**, 2754 (2004). *ibid,* J. Quant. Spectrosc. Radiat. Transfer, **99**, 225 (2006).
9. H. J. Lee, P. Neumayer, J. Castor, T. Döppner, R. W. Falcone, C. Fortmann, B. A. Hammel, A. L. Kritcher, O. L. Landen, R. W. Lee, D. D. Meyerhofer, D. H. Munro, R. Redmer, S. P. Regan, S. Weber, and S. H. Glenzer, Phys. Rev. Lett. **102**, 115001 (2009).
10. E. Garcia Saiz, G. Gregori, D. O. Gericke, J. Vorberger, B. Barbrel, R. J. Clarke, R. R. Freeman, S. H. Glenzer, F. Y. Khattak, M. Koenig, O. L. Landen, D. Neely, P. Neumayer, M. M. Notley, A. Pelka, D. Price, M. Roth, M. Schollmeier, C. Spindloe, R. L. Weber, L. van Woerkom, K. Wnsch, and D. Riley, Nature Physics **4**, 940 (2008).
11. A. L. Kritcher, P. Neumayer, J. Castor, T. Döppner, R. W. Falcone, O. L. Landen, H. J. Lee, R. W. Lee, E. C. Morse,1 Andrew Ng, S. Pollaine, D. Price, S. H. Glenzer, Science, **322**, 69 (2008).
12. S. Tzortzakis, P. Audebert, P. Renaudin, et al. J. Quan. Spectr. Trans. **99**, 614 (2006).
13. P. Beiersdorfer, et al., NIFS Proceedings Series No. NIFS-PROC-57, p. 40-46 (2004).
14. J. J. MacFarlane, et al., JQSRT **99**, 381-397 (2006).
15. L. Tonks and I. Langmuir, Phys. Rev. **33**, 195 (1929).
16. G. Gregori, A. Ravasio, A. Höll, S. H. Glenzer, and S. J. Rose, High Energy Den. Phys. **3**, 99 (2007).
17. A. L. Kritcher *et al*, *Manuscript in Preparation* (2009).